Available online at www.sciencedirect.com
SCIENCE DIRECT®
C. R. Physique 6 (2005) 888–896
COMPTES RENDUS PHYSIQUE
http://france.elsevier.com/direct/COMREN/

Spectroscopy and planetary atmospheres/Spectroscopie et atmosphères planétaires

Monitoring tropospheric pollution using infrared spectroscopy from geostationary orbit

Johannes Orphal [a,*], Gilles Bergametti [a], Benoît Beghin [b], Philippe-Jean Hébert [b], Tilman Steck [c], Jean-Marie Flaud [a]

[a] *LISA, CNRS and Universities of Paris-12 and Paris-7, 61, avenue du Général de Gaulle, 94010 Créteil, France*
[b] *CNES-Toulouse, 18, avenue Edouard Belin, 31401 Toulouse cedex 4, France*
[c] *Institut für Meteorologie und Klimaforschung, Forschungszentrum Karlsruhe, Postfach 3640, 76021 Karlsruhe, Germany*

Available online 5 October 2005

Abstract

This paper presents the Geostationary Fourier Imaging Spectrometer (GeoFIS), a new satellite instrument that has been proposed to monitor tropospheric key pollutants (O_3, CO) in order to improve the predictive capability of tropospheric chemistry models. The horizontal resolution of GeoFIS is about 15×15 km^2 and the temporal resolution is about 60 minutes. It is shown that the current instrument concept (based on available or under development optical, detector and platform technologies) is sufficient to provide tropospheric concentrations of O_3 and CO as well as columns of species like PAN with the required accuracies. ***To cite this article: J. Orphal et al., C. R. Physique 6 (2005).***

Résumé

Surveillance de la pollution troposphérique par spectroscopie infrarouge à partir d'une orbite géostationnaire. Dans cet article nous présentons le « Geostationary Fourier Imaging Spectrometer » (GeoFIS), un nouvel instrument satellite qui a été proposé pour surveiller les polluants troposphériques les plus importants (O_3, CO) afin d'améliorer la précision des prédictions fournies par les modèles de la chimie troposphérique. La résolution horizontale de GeoFIS est de 15×15 km^2 environ et la résolution temporelle est de 60 minutes. Nous montrons que le concept actuel de cet instrument (basé sur des technologies optiques, détecteur et plateforme disponibles ou en développement) est bien adapté pour fournir des concentrations troposphériques d'O_3 et de CO, ainsi que des colonnes d'espèces comme le PAN, avec les précisions requises. ***Pour citer cet article : J. Orphal et al., C. R. Physique 6 (2005).***

Keywords: Troposphere; Pollution; Air quality; Infrared; Spectroscopy; Geostationary orbit

Mots-clés : Troposphère ; Pollution ; Qualité de l'air ; Infrarouge ; Spectroscopie ; Orbite géostationnaire

* Corresponding author.
E-mail address: orphal@lisa.univ-paris12.fr (J. Orphal).

1631-0705/$ – see front matter
doi:10.1016/j.crhy.2005.09.003

1. Introduction

With the growing of the anthropogenic activities beginning at the end of the 19th century, air quality at local, regional and continental scales has become a major environmental issue. Until the end of the 1970s, air pollution mainly resulted from sulphur emissions from coal and fossil fuels [1]. These emissions of sulphur and associated particles were highest during winter when burning emissions were superimposed upon industrial activities. A well-known example of such sulphur pollution was the London smog event in December 1952 which lead to an excess of about 4000 deaths. Since then, due to the implementation of policies on SO_2 emissions, sulphur pollution events strongly decreased both in frequency and in intensity.

However, from the 1970s until now, air pollution problems have increased, due to the nitrogen oxides and volatile organic compounds (VOCs) that are mainly emitted into the atmosphere by vehicles. Since it was observed for the first time in Los Angeles, this type of air pollution was called the 'Los Angeles smog', but from a scientific point of view, it is photooxydant pollution, requiring photon energy provided by the solar ultraviolet (UV) radiation to initiate and maintain the chemical reactor [2]. More precisely, this pollution results from the oxidation in the atmosphere of the emitted VOCs in the presence of nitrogen oxides which generate, after complex chemical reactions, secondary products like ozone or fine particles. These secondary pollutants are suspected to be responsible for 30 000 additional deaths every year in Europe.

Briefly, this oxidation is initiated by various ways among which the most significant are the UV solar radiation (which breaks chemical bounds) and radicals like OH, NO_3 or the ozone itself. This oxidation evolves successively from VOCs to peroxy radicals (RO_2) and alkoxy radicals (RO) until all the organic carbon is transformed into CO_2. One of the major pathways of this oxidation process is the well-known 'Chapman cycle' [3]: in the troposphere, where the only available solar radiation is limited to wavelengths $\lambda > 290$ nm, nitrogen dioxide (NO_2) is the molecule that is the most easily photolysed. This photolysis produces NO and O. The latter recombines with molecular oxygen (O_2) to form an ozone molecule which can re-oxidize NO into NO_2.

Thus, one obtains a set of chemical reactions leading to a dynamic equilibrium between NO, NO_2 and O_3 which should actually lead to very low ozone concentrations. However a problem arises from the presence of peroxy radicals (as mentioned above they are a product of the oxidation of volatile organic compounds) which can also oxidize NO into NO_2 without consuming any ozone molecules, thus allowing the ozone to be accumulated into the troposphere.

In terms of air pollution management, the various air quality policies adopted either at national or European levels introduce various levels of alerts depending on the observed concentrations of the key pollutants. Furthermore they require the administrations to warn the population from the possible risks and to adopt measures to reduce the air pollution levels. In France, the '*Loi sur L'Air*' (Air Law) obliges the administrations to inform the population on the air quality over the whole national territory. Thus, they need both observational tools and numerical models to better assess and predict the concentrations of air pollutants.

The temporal, and thus also spatial, scales at which these processes occur are mainly dependent on the reactivity of the involved species. Most of them are very reactive, having lifetimes from only minutes to days, and thus the photooxydant plumes are frequently observed at 10–100 kilometers downwind the major cities and industrial areas. Significant spatial gradients are observed over limited areas. Moreover, due to the diurnal cycle of the solar irradiation and changes over the day of the emissions by traffic, air pollution exhibits very large spatial and temporal variability. Neither the ground based networks for air pollution nor the air quality forecast models can precisely assess in all situations the levels of air pollutants. Especially, the long-range transport of ozone plumes occurring in the free troposphere is not well accounted for by the ground based networks and the three-dimensional chemical models are strongly limited by the accuracy of the emission inventories. Providing frequent information over the whole European continent would significantly improve our capability of analysis and forecast of air pollution events. Satellite sensors, possibly in geostationary orbit, represent interesting new tools, in connection with ground based data and models, to progress towards an efficient operational air pollution management system.

The Geostationary Fourier Imaging Spectrometer (GeoFIS) instrument that is presented in this paper has first been proposed in 2002 [4]. GeoFIS has been entirely designed with the goal of monitoring key tropospheric pollutants, with the adequate temporal and spatial resolutions that are required to improve the accuracy of the predictions of tropospheric chemical models.

2. Infrared spectroscopy of the Earth's atmosphere

Observation of the Earth's atmosphere in the thermal infrared region (TIR, corresponding to wavelengths of about 4–16 microns) has the main advantage that the source of signal is the thermal emission of the Earth's surface and of the lowest atmospheric layers (corresponding to blackbody radiation at about 300 K), so that observations are possible during day and night [5]. A typical spectrum of the Earth (Nadir observation geometry), calculated with the LBLRTM model [6] is shown in Fig. 1. The absorption features of many important atmospheric trace gases (O_3, CO, CO_2, H_2O, CH_4 and N_2O) are easily identified. Together with spectroscopic data from high-resolution databases (e.g., HITRAN [7] or GEISA [8]), atmospheric concentrations of these gases can be determined using radiative transfer models and associated retrieval codes [9]. The vertical

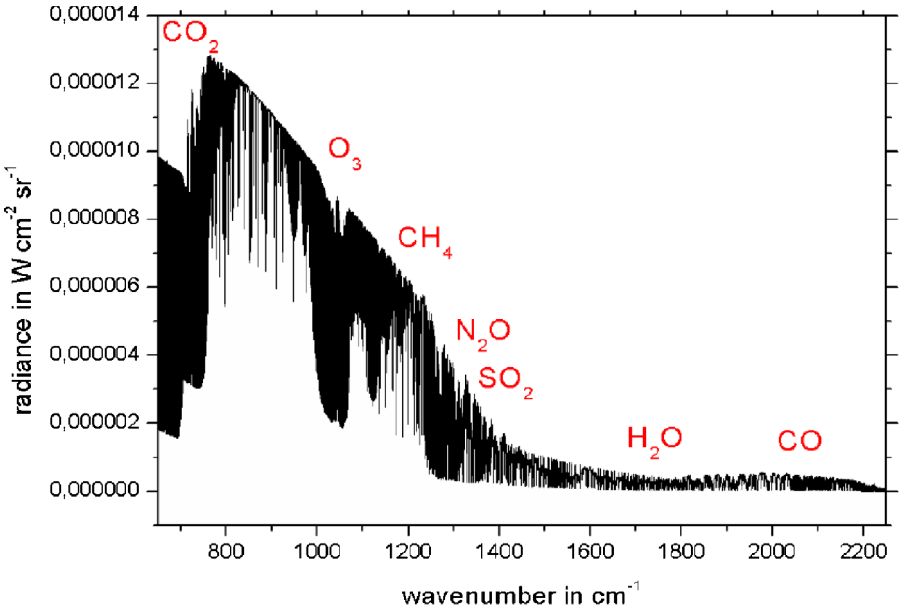

Fig. 1. Infrared spectrum of the Earth. This figure shows the emission spectrum of the Earth atmosphere in the mid-infrared region (700–2250 cm^{-1}) calculated with the radiative transfer model LBLRTM for mid-latitude conditions (summer, unpolluted scenario). The most important absorption bands of different trace gases (O_3, CO, CO_2, H_2O, CH_4, N_2O) are indicated.

information can be obtained from the different transparency of the atmosphere at different wavelengths, from the pressure-dependence of the widths of molecular absorption lines and from the temperature-dependence of the individual line intensities (due to the thermal population of the quantized rotational-vibrational energy levels). For the latter reference data, accurate laboratory measurements and sophisticated theoretical models are essential, in order to reproduce high-resolution atmospheric spectra within the experimental uncertainties [10].

Previous infrared Nadir-looking satellite instruments (the 'Interferometric Monitor of Greenhouse Gases' IMG operated on the Japanese 'ADEOS' platform in 1997–98 [11] and the 'Tropospheric Emission Spectrometer' TES operated on the U.S. 'EOS-Aura' platform launched in 2004 [12]) have clearly demonstrated the capability of measuring tropospheric trace gases using infrared emission spectra, a concept that has first been proposed in 1995 [13]. However, since these platforms are flying in polar sun-synchronous orbits (altitude of about 800 km, so-called 'low-Earth orbits'), the temporal coverage of these previous instruments is limited to a revisit time of about three days. Possibilities to improve the temporal coverage are either a fleet of several satellites in classical low-Earth orbits (for a global Earth coverage), one to three satellites in drifting low-Earth orbits (for a better regional coverage) or one satellite in a geostationary orbit (altitude of 36 000 km), at the cost of loosing the global Earth coverage. Based on the latter, the Geostationary Fourier Imaging Spectrometer (GeoFIS) has first been proposed to the European Space Agency (ESA) in 2002 [14] as part of the Geostationary Tropospheric Pollution Explorer (GeoTroPE) mission [4].

3. Observational and data requirements

From recent studies [15,16], the most important pollutants that need to be monitored in order to improve the predictive capability of tropospheric chemistry models are NO_2, CO, O_3, H_2CO, PAN (acronym for PeroxyAcetylNitrate, $CH_3C(O)OONO_2$) and organic species such as C_2H_6. The temporal resolution of the observations should be better then 2 hours (goal 30 minutes) and the horizontal resolution should be better than 20×20 km^2 (goal 5×5 km^2) with a pointing accuracy of about 10% of the size of a ground pixel to account for the high spatial and temporal variability of the trace gases concentrations. The vertical resolution should be high enough to provide tropospheric columns of these trace gases (threshold) or even information on their concentration in different tropospheric layers, with particular interest in observing trace gas concentrations in the lowest part of the troposphere, the so-called 'Planetary Boundary Layer' (PBL, about 0–2 km altitude). Other parts of interest for the troposphere are the so-called 'lower troposphere' (LT, about 2–7 km) and 'upper troposphere' (UT, about 7–15 km). Note that all these layers are variable in height as a function of seasonal and meteorological conditions.

In the last 5 years, significant effort has been made to develop an instrument concept that fulfils these rather demanding requirements. In the following paragraphs, the sensitivity studies that were carried out for the GeoFIS project and the current instrument concept will be presented.

4. Sensitivity studies and instrument requirements

For the calculations presented here, the 'Karlsruhe Optimized and Precise Radiative transfer Algorithm' (KOPRA) [17] was used as forward radiative transfer model (RTM) including the calculation of derivatives (Jacobians) that are needed for the retrieval of atmospheric concentration profiles from infrared atmospheric spectra.

KOPRA is a Fortran-90 computer code for atmospheric radiative transfer modeling in the mid-infrared spectral range. It has been developed as a self-standing algorithm including all relevant physics from the troposphere to the thermosphere as well as the instrument specific response function of the Michelson Interferometer for Passive Atmospheric Sounding (MIPAS/ENVISAT) experiment [18] besides other more standard ones. KOPRA is based on high level physical algorithms, in order to give optimum solutions and their realizations for the relevant problems within the sub-tasks of radiative transfer modeling. In particular, these are the set-up of the geophysical model and the stratification of the atmosphere, the atmospheric ray path modeling, the calculation of absorption coefficients on an optimized wavenumber grid, the treatment of line-mixing, the consideration of absorption and emission of heavy molecules and of continua caused by gaseous constituents and solid particles, and the radiative transfer integration along the line of sight including the treatment of effects caused by non-local thermodynamic equilibrium (NLTE) [19]. In each part of KOPRA, optimizations have been taken into account as long as they are not on the cost of accuracy or flexibility, in order to provide a tool suitable for the analysis of numerous data in an automated retrieval set-up. KOPRA also includes the modeling of the instrumental response function in terms of instrumental line shape and the effect of finite field of view, both for the particular MIPAS/ENVISAT design details, and for more standard-designed instruments.

Using KOPRA and its associated retrieval code, the following parameters were varied in order to derive an optimum instrument concept for GeoFIS in order to fulfill the observational and data requirements:

- spectral coverage,
- spectral resolution,
- signal-to-noise ratio.

The number of degrees of freedom (vertical layers) in the troposphere was fixed to three, using so-called first-order Tikhonov constraints [9,20], corresponding to the three layers of interest (PBL, LT and UT). Such calculations were not carried out for NO_2 and H_2CO since these species, although in principle present in TIR spectra, absorb only very weakly and are heavily masked by H_2O lines [13,21]. In addition they are more easily observed using UV-visible instruments [22,23].

The obtained GeoFIS instrument requirements are summarized in Table 1, where the spectral coverage, spectral resolution, and noise-equivalent differential temperature (NEDT) are given. One can see that the spectral coverage can be divided into two bands focusing on O_3, PAN, and CO, with an (optional, see below) third channel focusing on C_2H_6. In the first column, the corresponding GeoFIS channel name is given. The 'goal' and 'threshold' specifications for the signal-to-noise ratio correspond to the different requirements on the accuracy of trace gas concentrations [15].

Table 2 shows the results of synthetic retrievals of O_3 and CO (GeoFIS channels B2 and B4) for a ground pixel size of 15×15 km^2, and spectral resolutions (apodized) of 0.25 cm^{-1} and 0.50 cm^{-1} in Channels B2 and B4, respectively. The three tropospheric layers (PBL, LT, UT) correspond to the altitude ranges 0–2 km (PBL), 2–7 km (LT) and 7–15 km (UT), respectively. One can see that for Channel B2, a signal-to-noise ratio of 1200 is required to retrieve O_3 in the lowest layer (PBL) with an accuracy of about 50%. For Channel B4, a signal-to-noise ratio of 450 is required to retrieve CO in the lowest layer (PBL) with an accuracy of about 35%. These calculations are very important to define the instrument parameters as discussed in the next section.

Note that in addition, the influence of the thermal contrast (i.e., the temperature difference between the surface and the lowest atmospheric layer) was studied. The strong impact of thermal contrast is illustrated in Fig. 2 where in the RTM calculations with KOPRA, the temperature of the lowest layer of the atmosphere was 'kept' at 280 K while the temperature of the surface was varied between 270 K and 300 K. The impact on the retrieval accuracy is shown in Table 3 (calculated for a signal/noise ratio of 1200 and a spectral resolution of 0.25 cm^{-1}). One can clearly see that for low thermal contrast (lowest atmospheric layer 'kept' at 280 K) the retrieval is not very accurate (uncertainty of 52% in the PBL) but that a small change in the thermal contrast of

Table 1
GeoFIS requirements

Channel	Coverage (cm^{-1})	Resolution (cm^{-1})	Target species	NEDT goal (K)	NEDT threshold (K)	Comment
B2	975–1200	0.25	O_3, PAN	0.017	0.037	
B4	2100–2200	0.50	CO	0.050	0.050	
B1	800–850	0.25	C_2H_6	0.023	0.047	Optional

Table 2
GeoFIS performance

O_3 (GeoFIS Channel B2, resolution 0.25 cm^{-1})				
Signal/noise ratio	Error PBL (%)	Error LT (%)	Error UT (%)	Mean vertical resolution (km)
4800	13.1	6.0	3.1	6.2
2400	26.1	11.9	6.2	6.2
1200	52.0	23.6	12.3	6.2
600	105.0	47.5	24.8	6.2

CO (GeoFIS Channel B4, resolution 0.50 cm^{-1})				
Signal/noise ratio	Error PBL (%)	Error LT (%)	Error UT (%)	Mean vertical resolution (km)
900	17.2	7.6	7.4	6.0
450	34.6	15.4	15.0	6.0
225	68.6	30.4	29.6	6.0
120	128.0	56.7	55.2	6.0

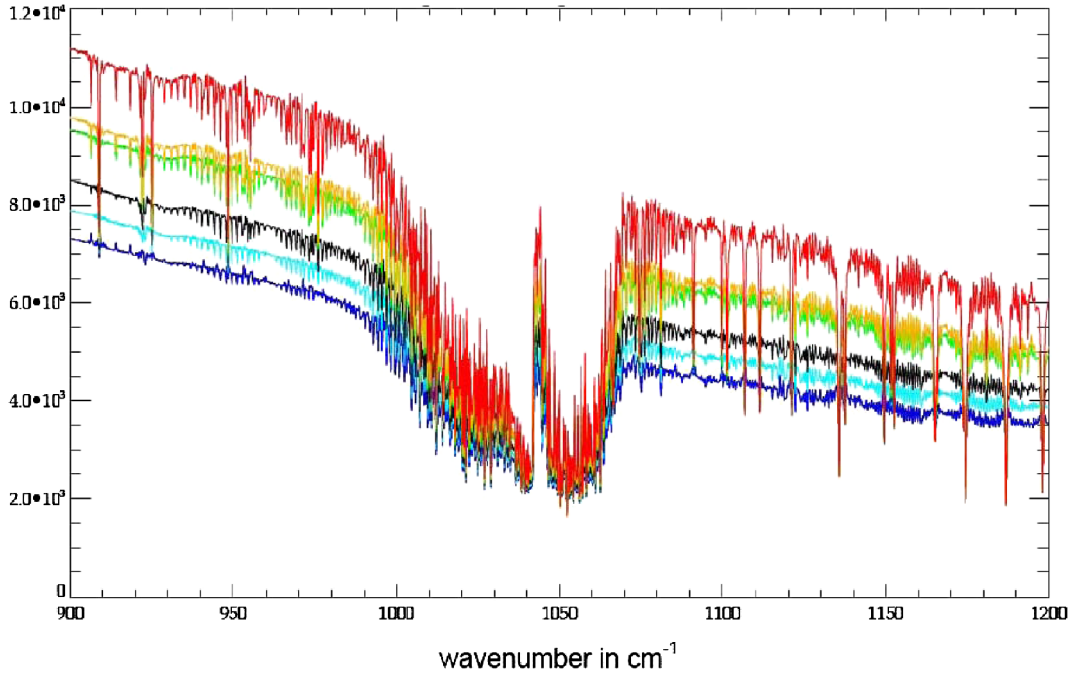

Fig. 2. GeoFIS Channel B2. This figure shows the influence of the surface temperature in the ozone band region (900–1200 cm^{-1}, corresponding to Channel B2 of the GeoFIS instrument) calculated with the radiative transfer model KOPRA. The spectral resolution and signal-to-noise ratio of the GeoFIS instrument are included in the simulation. The curves (from top to bottom) were obtained for surface temperatures of 300 K (red), 290 K (yellow), 288 K (green), 280 K (black), 275 K (light blue), and 270 K (dark blue), respectively. Note the strong variation of the total signal. Absorption lines outside the 980–1090 cm^{-1} region are due to H_2O, CO_2, CH_4 and N_2O. (For interpretation of the references to color in this figure, the reader is referred to the web version of this article.)

only 5–8 K will significantly improve the accuracy of the retrievals by about a factor of two (19 and 29%, respectively, for 275 K and 288 K). Note also that in the calculations presented in Table 2, a low thermal contrast was assumed (surface temperature of 280 K), so that the expected accuracy of the GeoFIS data will be higher for most situations.

A difficult parameter is the mean vertical resolution in Tables 2 and 3 which corresponds to the full-width at half-maximum of the diagonal elements of the averaging kernel matrix. It indicates the correlations between different altitudes, and one can clearly see that for the lowest layer (PBL), there is also information from the second layer (LT) that influences the results.

Table 3
GeoFIS performance: impact of thermal contrast

O_3 (GeoFIS Channel B2, resolution 0.25 cm^{-1}, signal/noise ratio 1200)				
Surface temperature (K)	Error PBL (%)	Error LT (%)	Error UT (%)	Mean vertical resolution (km)
270	8.6	7.5	4.8	6.3
275	18.8	11.4	5.5	5.7
280	52.0	23.6	12.3	6.3
288	29.4	16.2	14.2	5.5
290	26.2	14.5	13.2	5.6
300	19.5	11.9	12.2	6.1

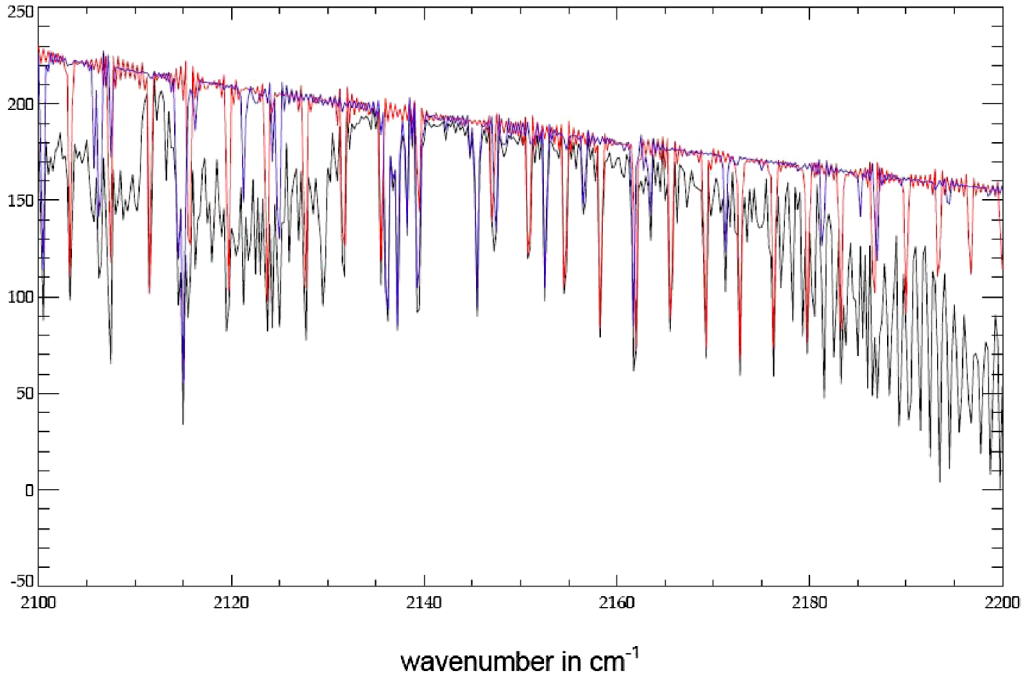

Fig. 3. GeoFIS Channel B4. This figure shows the influence other trace gases in the CO region (2100–2200 cm^{-1}, corresponding to Channel B4 of the GeoFIS instrument) calculated with the radiative transfer model KOPRA. From top to bottom the different curves were obtained for CO only (red), H_2O only (blue), and for all molecules (including also CO_2, N_2O, O_3, and CH_4) (black). The spectral resolution and signal-to-noise ratio of the GeoFIS instrument are included in the simulation. This simulation illustrates the importance of selecting appropriate micro-windows in order to minimize the influence of interfering species. (For interpretation of the references to color in this figure, the reader is referred to the web version of this article.)

Finally, the accuracy of vertical temperature profiles also has an important impact on the retrieval accuracy, mainly because different lines and different molecules contribute to the signal received in the various spectral channels. These effects can be in some way minimized by selecting spectral 'micro-windows' [24,25] which are highly sensitive to the atmospheric parameter that shall be determined and at the same time least sensitive to other parameters (temperature, other species). However the impact of the uncertainty of vertical temperature profiles always exists. For the numbers given in Table 1, the accuracy of vertical temperature profiles has to be 0.5 K (goal) to 1.0 K (threshold) in order to be negligible. For the GeoFIS project, it is important to stress that such data should be available from operational meteorological services within the next years [26].

5. GeoFIS instrument concept and parameters

The GeoFIS instrument concept and parameters have been established in 2002–2005 by collaboration between scientists from CNRS–LISA (France) and IMK–FZK (Germany) and the 'PASO' team of the French Space Agency (CNES) in Toulouse

Table 4
GeoFIS parameters

GeoFIS parameters	Values
Dwell time	$\sim 4 \times 3$ s
Spatial sampling (Nadir)	15×15 km^2 pixel size N/S and E/W
Spatial coverage (staring mode)	70–15° N $\leftrightarrow$ 256 pixels 15°W–60°E $\leftrightarrow$ 320 pixels
Dimensions (cm)	$120 \times 60 \times 45$ cm^3
Mass estimate, total	120–150 kg (conservative)
Power estimate, total (W)	250 W
Transmission data rate	less than 700 Mbit/s (goal 300 Mbit/s)
Instrument mechanism	scanning FTS (3.2 s acquisition time)
Pointing knowledge pitch/roll/ yaw (1σ)	4.3/4.3/25 arcsec. (12 s)
Pointing stability pitch/roll/ yaw (1σ)	8.6/8.6/45 arcsec. (12 s)

(France). Two different instrument concepts were studied [27]: a grating spectrometer and a Fourier-transform spectrometer. It was clearly shown that the dimensions of a grating spectrometer would be significantly too high to be operational on a geostationary orbit and that an infrared Fourier-transform spectrometer was feasible. Such spectrometers have indeed been successfully operated in space onboard the Space Shuttle (the ATMOS/ATLAS project [28]) and on the ADEOS (IMG [29]), ENVISAT (MIPAS [18]), SCISAT (ACE-FTS [30]) and EOS-AURA (TES [12]) satellite platforms. The 'Infrared Atmospheric Sounding Instrument' (IASI [31]) is currently being prepared for launch on the EUMETSAT 'MetOp' series of satellites (launch planned for mid-2006).

Finally the instrument that would best meet the requirements previously given is a scanning Fourier-transform spectrometer (based on the IASI design) with a maximum optical path difference of 4 cm (which is two times higher than that used for the IASI instrument), with an entrance optics (without telescope) estimated at a 5 cm diameter, and with two large focal plane array (LFPA) detectors derived from technologies that are commercially available (Sofradir France), with 320×256 pixels each. The detector temperature will be about 80 K that may be achieved using passive coolers (except for the optional Channel B1 that requires a temperature of ~ 55 K). The threshold signal/noise ratios given in Table 1 can be achieved with such an instrument in 30 minutes of atmospheric measurement time, with one interferogram in each channel measured each 3 seconds. The data from the two LFPA detectors will be digitized (12 bit in Channel B2 and 9 bit in Channel B4), averaged over four interferograms (about 12 seconds), compressed and inspected for cloud contamination (see below) and pointing stability, before being sent down to the ground station (with a data rate not exceeding 700 Mbit/second, the goal being to reduce the downlink data rate to about 300 Mbit/second).

The most important instrument parameters of GeoFIS are given in Table 4, and a schematic view of the GeoFIS instrument is shown in Fig. 4. It is important to note that the instrument design is based on available technologies for most components (IASI-type optics together with commercially available LFPA detectors) that are already space qualified, but its high performance requirements make it a still challenging system to settle.

In addition to the nominal viewing mode (Earth), the TIR instrument needs two additional modes for in-orbit radiometric calibration: pointing to an on-board blackbody source (maintained stable at a temperature of 300 K) and to cold space. This is achieved with a switch mirror (see Fig. 4) that in standard mode points to the Earth (Europe). The time allocated for radiometric calibration is 30 minutes per hour. Also the instrument has to be protected by a baffle (see Fig. 4) against direct light from the Sun that would have a strong impact on thermal and radiometric parameters.

An important problem is the possible contamination of the measured signal by clouds. In a recent study [32], it was shown that on average, during 30 minutes of observation, about 30% of the ground pixels (size 15×15 km^2) are fully free of clouds. At this point it should be stressed that, as discussed in the first section of this paper, sunlight is essential in order to maintain the chemical reactions leading to pollution, so that cloud-free pixels are the most interesting ones from the chemical point of view. It is probably possible to identify the presence of clouds directly using the infrared signal so that no additional cloud detector is required, although a high-resolution imager operating in the visible and/or near-infrared would probably help to identify cloud contamination. These problems are currently being discussed and need further investigation.

6. Conclusions and outlook

In this paper, we have described the scientific problems and the technical aspects of the GeoFIS project that proposes to monitor tropospheric air quality from a geostationary orbit. It has been shown that such an instrument can be developed mainly based on currently available components and technology, and that this challenging instrument will provide the data required to improve the predictive capability of tropospheric chemical models. GeoFIS is currently proposed to ESA to fly together with

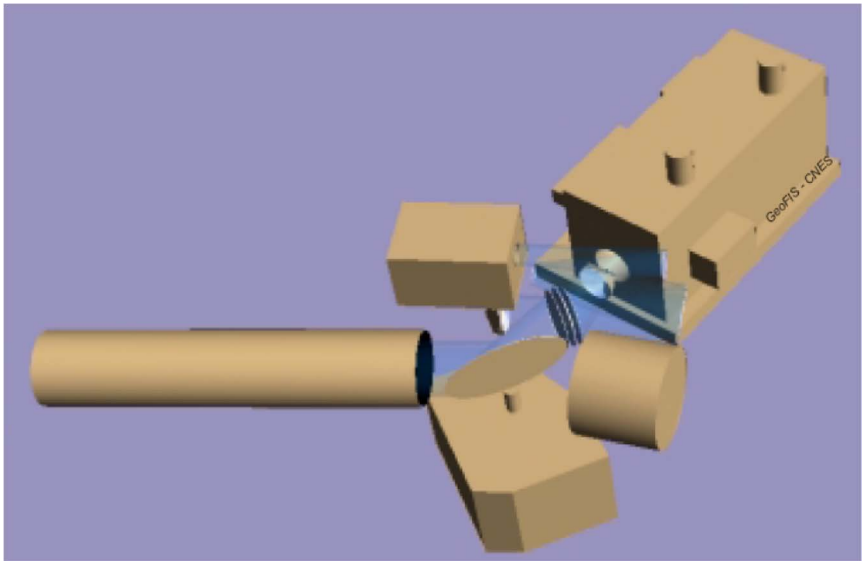

Fig. 4. Sketch of the GeoFIS instrument. This figure shows a sketch of the GeoFIS instrument (courtesy CNES Toulouse). The photons from the Earth pass first through the entrance baffle (protecting the instrument against solar radiation) on the left-hand side, and are then directed via a switch mirror (required to point to cold deep space and to the 300 K blackbody source for radiometric calibration, the cylindrical body right to the baffle) to the interferometer (right upper part of the image). The control laser is included in the box of the interferometer. The overall dimensions of the instrument are 1.20 m × 0.60 m × 0.45 m.

the UV-visible GeoSCIA instrument [23] on the GeoTroPE mission [4] as a prototype for operational tropospheric chemistry monitoring, a segment that will be an essential component of the European 'Global Monitoring for Environment and Security' (GMES) initiative [33].

Acknowledgements

We thank warmly the following colleagues whose inputs have been valuable for this paper: M. Beekmann, N. Blond, H. Bovensmann, J.P. Burrows, P. Chelin, I. Coll, H. Fischer, F. Friedl-Vallon, F. Gonzalez, H. Oelhaf, V.-H. Peuch, G. Stiller, and Th. von Clarmann. Part of the work presented in this paper was supported by the French Space Agency CNES ('TOSCA' programme), by the European Space Agency ESA/ESTEC ('CAPACITY' study), and by the European Network of Excellence on Atmospheric Composition Change 'ACCENT–TROPOSAT-2'.

References

[1] P.A. Leighton, Photochemistry of Air Pollution, Academic Press, New York, 1961.
[2] B. Finlayson-Pitts, Chemistry of the Upper and Lower Atmosphere, Academic Press, New York, 1999.
[3] J. Seinfeld, S.N. Pandis, Atmospheric Chemistry and Physics: From Air Pollution to Climate Change, John Wiley and Sons, New York, 1997.
[4] J.P. Burrows, H. Bovensmann, G. Bergametti, J.-M. Flaud, J. Orphal, S. Noel, P.S. Monks, G.K. Corlett, A.P. Goede, T. von Clarmann, T. Steck, H. Fischer, F. Friedl-Vallon, The Geostationary Tropospheric Pollution Explorer (GeoTROPE) mission: objectives and requirements, Advances in Space Research 34 (2004) 682–687.
[5] R. Beer, Remote Sensing by Fourier Transform Spectrometry, John Wiley and Sons, New York, 1992.
[6] S.A. Clough, M.W. Shephard, E.J. Mlawer, J.S. Delamere, M.J. Iacono, K. Cady-Pereira, S. Boukabara, P.D. Brown, Atmospheric radiative transfer modelling: a summary of the AER codes, Journal of Quantitative Spectroscopy and Radiative Transfer 91 (2005) 233–244.
[7] L.S. Rothman, D. Jacquemart, A. Barbe, D.C. Benner, M. Birk, L.R. Brown, M.R. Carleer, C. Chackerian Jr., K.V. Chance, V. Dana, V.M. Devi, J.-M. Flaud, R.R. Gamache, A. Goldman, J.-M. Hartmann, K.W. Jucks, A.G. Maki, J.-Y. Mandin, S. Massie, J. Orphal, A. Perrin, C.P. Rinsland, M.A.H. Smith, R.A. Toth, J. Vander Auwera, P. Varanasi, G. Wagner, The HITRAN 2004 molecular spectroscopic database, Journal of Quantitative Spectroscopy and Radiative Transfer 96 (2005) 139–204.
[8] N. Jacquinet-Husson, E. Arie, J. Ballard, A. Barbe, G. Bjoraker, B. Bonnet, L.R. Brown, C. Camy-Peyret, J.P. Champion, A. Chedin, A. Chrusin, C. Clerbaux, G. Duxbury, J.-M. Flaud, N. Fourrie, A. Fayt, G. Graner, R. Gamache, A. Goldman, V. Golovko, G. Guelachvili,

J.-M. Hartmann, J.C. Hilico, J. Hillman, G. Lefevre, E. Lellouch, S.N. Mikhailenko, O.V. Naumenko, V. Nemtchinov, D. Newnham, A. Nikitin, J. Orphal, A. Perrin, D.C. Reuter, C.P. Rinsland, L. Rosenmann, L.S. Rothman, N.A. Scott, J. Selby, L.N. Sinitsa, J.M. Sirota, A.M. Smith, K.M. Smith, V.G. Tyuterev, R.H. Tipping, S. Urban, P. Varanasi, M. Weber, The 1997 spectroscopic GEISA databank, Journal of Quantitative Spectroscopy and Radiative Transfer 62 (1999) 205–254.

[9] C.D. Rodgers, Inverse Methods for Atmospheric Sounding: Theory and Practice, World Scientific, Singapore, 2000.

[10] J.-M. Flaud, H. Oelhaf, Infrared spectroscopy and the terrestrial atmosphere, Comptes Rendus de l'Académie des Sciences (Paris) 5 (2004) 259–271.

[11] C. Clerbaux, P. Chazette, J. Hadji-Lazaro, G. Mégie, J.-F. Moeller, S.A. Clough, Remote sensing of CO, CH_4 and O_3 using a space-borne nadir-viewing interferometer, Journal of Geophysical Research D 108 (1998) 18999–19013.

[12] R. Beer, T.A. Glavich, D.M. Rider, Tropospheric emission spectrometer for the Earth Observing System's Aura satellite, Applied Optics 40 (2001) 2356–2367.

[13] G. Wetzel, H. Fischer, H. Oelhaf, Remote sensing of trace gases in the mid-infrared spectral region from a nadir view, Applied Optics 34 (1995) 467–479.

[14] J.-M. Flaud, J. Orphal, G. Bergametti, C. Deniel, Th. von Clarmann, F. Friedl-Vallon, T. Steck, H. Fischer, H. Bovensmann, J.P. Burrows, M. Carlotti, M. Ridolfi, L. Palchetti, The Geostationary Fourier Imaging Spectrometer (GeoFIS) as part of the Geostationary Tropospheric Pollution Explorer (GeoTROPE) mission: objectives and capabilities, Advances in Space Research 34 (2004) 688–693.

[15] H. Kelder, et al., Composition of the Atmosphere: Progress to Applications in the user CommunITY (CAPACITY), Final report to ESA, Noordwijk, 2005.

[16] J. Lelieveld, Geostationary satellite observations for monitoring atmospheric composition and chemistry applications, Final report to EUMETSAT, Darmstadt, 2003.

[17] The Karlsruhe Optimized and Precise Radiative transfer Algorithm (KOPRA), G.P. Stiller (Editor) with contributions from T. von Clarmann, A. Dudhia, G. Echle, B. Funke, N. Glatthor, F. Hase, M. Höpfner, S. Kellmann, H. Kemnitzer, M. Kuntz, A. Linden, M. Linder, G.P. Stiller, S. Zorn, Forschungszentrum Karlsruhe, Wissenschaftliche Berichte, Bericht Nr. 6487, 2000.

[18] T. von Clarmann, T. Chidiezie Chineke, H. Fischer, B. Funke, M. García-Comas, S. Gil-López, N. Glatthor, U. Grabowski, M. Höpfner, S. Kellmann, M. Kiefer, A. Linden, M. López-Puertas, M.Á. López-Valverde, G. Mengistu Tsidu, M. Milz, T. Steck, G.P. Stiller, Remote sensing of the middle atmosphere with MIPAS, in: K. Schäfer, O. Lado-Bordowsky, A. Comerón, R.H. Picard (Eds.), Remote Sensing of Clouds and the Atmosphere, vol. VII, in: Proceedings of SPIE, vol. 4882, SPIE, Bellingham, WA, 2003, pp. 172–183.

[19] M. López-Puertas, B. Funke, M.A. López-Valverde, F.J. Martín-Torres, T. v. Clarmann, G.P. Stiller, H. Oelhaf, H. Fischer, J.-M. Flaud, Non-LTE studies for the analysis of MIPAS–ENVISAT data, in: K. Schäfer, O. Lado-Bordowsky, A. Comerón, M.R. Carleer, J.S. Fender (Eds.), Remote Sensing of Clouds and the Atmosphere, vol. VI, in: Proceedings of SPIE, vol. 4539, SPIE, 2002, pp. 381–395.

[20] T. Steck, Methods for determining regularization for atmospheric retrieval problems, Applied Optics 41 (2002) 1788–1797.

[21] C. Clerbaux, P.-F. Coheur, J. Hadji-Lazaro, S. Turquety, Capabilities of infrared sounder observations for monitoring atmospheric composition and chemistry applications, Final report to EUMETSAT, Darmstadt, 2003.

[22] H. Bovensmann, M. Buchwitz, S. Noël, K.-U. Eichmann, V. Rozanov, J.P. Burrows, J.-M. Flaud, G. Bergametti, J. Orphal, P. Monks, G. Corlett, A.P. Goede, Th. von Clarmann, F. Friedl-Vallon, T. Steck, H. Fischer, Sensing of air quality from geostationary orbit, in: Proceedings of the 2002 EUMETSAT Meteorological Satellite Conference, EUMETSAT, Darmstadt, 2003, pp. 89–96, ISBN 92-9119-049-8.

[23] H. Bovensmann, K.-U. Eichmann, S. Noel, J.-M. Flaud, J. Orphal, P.S. Monks, G.K. Corlett, A.P.H. Goede, T. von Clarmann, T. Steck, V. Rozanov, J.P. Burrows, The GeoStationary Scanning Imaging Absorption Spectrometer (GeoSCIA) as part of the GeoStationary Tropospheric Pollution Explorer (GeoTROPE) mission: requirements, concepts and capabilities, Advances in Space Research 34 (2004) 694–699.

[24] A.A. Dudhia, V.L. Jay, C. Rodgers, Microwindow selection for high-spectral-resolution sounders, Applied Optics 41 (2002) 3665–3673.

[25] J. Worden, S.S. Kulawik, M.W. Shephard, S.A. Clough, H.A. Worden, K. Bowman, A. Goldman, Predicted errors of tropospheric emission spectrometer nadir retrievals from spectral window selection, Journal of Geophysical Research 109 (2004) D09308, doi:10.1029/2004JD004522.

[26] V.-H. Peuch, Personal communication, 2005.

[27] P.-J. Hebert, Phase 0 GeoFIS: Synthèse et dimensionnement, CNES document Ref. DCT/SI/IN/2005-051, Toulouse, 2005.

[28] C.B. Farmer, High resolution infrared spectroscopy of the Sun and the Earth's atmosphere from space, Mikrochim. Acta Wien III (1987) 189–214.

[29] H. Kobayashi (Ed.), Interferometric Monitor for Greenhouse Gases (IMG), Project Technical Report, Central Research Institute of Electric Power Industry, Komae Research Laboratory, Atmospheric Science Department, Tokyo, Japan, 1999.

[30] P.F. Bernath, et al., Atmospheric Chemistry Experiment (ACE): Mission overview, Geophysical Research Letters 32 (2005) L15S01, doi:10.1029/2005GL022386.

[31] D. Blumstein, G. Chalon, T. Carlier, C. Buil, P. Hébert, T. Maciaszek, G. Ponce, T. Phulpin, B. Tournier, D. Siméoni, IASI instrument: Technical overview and measured performances, SPIE 2004-5543-22, 2004.

[32] F. Rocher, T. Phulpin (CNES), Etude de la nébulosité, personal communication, 2005.

[33] Establishing a GMES capacity by 2008 (Action Plan (2004–2008)), Communication from the Commission to the European Parliament and the Council, EU COM/2004/65, Brussels, 2004.